Materials Advances

ROYAL SOCIETY OF CHEMISTRY

REVIEW

View Article Online
View Journal | View Issue

Cite this: *Mater. Adv.*, 2023, 4, 374

Recent advances in green thermally activated delayed fluorescence emitters towards high colour purity and good electroluminescence performance

Ramanaskanda Braveenth, [ab] Kanthasamy Raagulan,[ab] Yu-Jin Kim[b] and Bo-Mi Kim*[b]

The conventional donor–acceptor (D–A) and donor–acceptor–donor (D–A–D) types of thermally activated delayed fluorescence (TADF) emitters manifested excellent electroluminescence efficiencies in recent years. However, the color purity of these emitters is not satisfactory due to the enhanced charge transfer characteristics. Such broad emission spectra with wide full width at half maximum (FWHM) must be narrowed down for their potential implementation in ultrahigh-definition display technology. Recently, polycyclic aromatic molecular skeleton-based emitters, specified as multi resonance (MR) type of TADF emitters, have drawn immense attention due to the achievable high color purity required by the standard. However, making bathochromic shifted and controlled emission (green) using a polycyclic aromatic core is identified as one of the challenging parts of molecular designing. Several strategies are implemented towards the development of green emitters without affecting the electroluminescence efficiencies. This review focuses on the recent progress of green emitters from the perspective of molecular design strategy and electroluminescence performance, offering a brief overview of highly efficient conventional green TADF emitters and MR-TADF emitters. Conventional green TADF emitters are selected to discuss their device performance corresponding with the molecular design evolution. At the same time, MR-TADF types of green emitters are comprehensively discussed due to their inherent need in future display technology.

Received 12th October 2022,
Accepted 22nd November 2022

DOI: 10.1039/d2ma00967f

rsc.li/materials-advances

[a] *Division of Bio-Nanochemistry, College of Natural Sciences, Wonkwang University, Iksan 570-749, Korea*
[b] *Department of Chemical Engineering, Wonkwang University, Iksan 570-749, Korea. E-mail: 123456@wku.ac.kr*

Ramanaskanda Braveenth

Dr Ramanaskanda Braveenth received his PhD degree in Chemistry from Wonkwang University (Republic of Korea) in 2020 under the supervision of Prof. Kyu Yun Chai. During his PhD, he worked on developing novel organic materials for OLED applications. During 2020–2022, he was a research professor under Prof. Jang Hyuk Kwon at the Department of Information display of Kyung Hee University (Republic of Korea). His research interest encompasses the design of new blue and green TADF emitters for optoelectronic device applications.

Kanthasamy Raagulan

Dr Kanthasamy Raagulan received his BSc (Hons) in Chemistry from the University of Jaffna (UOJ), Sri Lanka and completed his MSc in Nanoscience and Nanotechnology from the Post Graduate Institute of Science (PGIS), University of Peradeniya, Sri Lanka. He finished his PhD degree in Chemistry from Wonkwang University, Republic of Korea (2021), under the supervision of Prof. Kyu Yun Chai. During his PhD, he worked on developing MXene nanocomposites for electromagnetic interference shielding (EMI-SE) applications. His current research focuses on the development of semiconductor quantum dots for various applications.

Introduction

The development of primary colors for the application in organic light emitting diode (OLED) displays became a matter of contention over the past 25 years. The evolution of emitting materials passed through various phases of design approaches. The first-generation emitters utilized only singlet excitons of 25% internal quantum efficiency (IQE), which led to poor device efficiencies.[1–3] The successful achievement of 100% IQE was enabled in second generation phosphorescence emitters, where noble heavy metals of iridium and platinum were used as core materials coordinated with various types of ligands and activated spin orbital coupling (SOC) facilitated to harvest 25% singlet excitons to triplet excitons *via* an inter system crossing mechanism.[4–10] Since then phosphorescence emitters have marched towards the accomplishment of highly efficient OLED devices and have been applied in commercial display products. However, they raised concerns regarding the cost of rare heavy metals and environmental issues set back the wide application of phosphorescence emitters in commercial markets.[11,12]

To overcome the obstacles associated with second generation emitters, third generation emitters were proposed by Adachi *et al.* Hereafter, thermally activated delayed fluorescence (TADF) emitters drew great recognition from the scientific community due to their advantages, such as heavy metal free molecular skeleton, reaching a theoretical maximum of 100% IQE and versatile molecular building blocks.[13,14] Since TADF has become the third-generation dopants for OLEDs, the design of TADF molecules also set off together with the development. TADF mechanism is mainly dependent on the reverse intersystem crossing (RISC), which helps to up covert the dark triplet excitons to radioactive singlet excitons.[15–17] However, such a process is possible when the energy gap difference between the excited singlet and triplet states (ΔE_{ST}) becomes small. To obtain a small ΔE_{ST} in an organic molecular framework, the presence of donor (D) and acceptor (A) moieties in a single molecule is a requisite. D–A type molecules manifest the intra molecular charge transfer (ICT) characteristics through the separation of the frontier molecular orbital (FMO) distributions. FMO separation is possible when a D–A type molecule possesses a twisted molecular skeleton. At the same time, a certain degree of rigidity is also an important factor in maintaining high photoluminescence quantum yield (PLQY), which directly influences the efficiency of OLED devices.[18–20]

At the initial stage of TADF development, blue and red emitters were given much attention due to their challenging molecular design strategy. At the same time, various design strategies are being applied to green TADF emitters while considering good TADF properties and high PLQY. To fulfill such requirements, several combinations of donor and acceptor moieties are adopted, such as strong donor–weak acceptor, weak donor–strong acceptor, and moderate donor and acceptors. The above mentioned combinations can be used to design a green emitter possessing good TADF performances by lowering the ΔE_{ST} and enhancing the intramolecular charge transfer characteristics.[21,22]

Early development of green TADF emitters utilized cyano and triazine acceptor moieties due to their strong electron withdrawing nature. Not only limited to cyano and triazine acceptors, but also researchers have put tremendous effort into designing green TADF emitters incorporating numerous acceptor moieties, such as pyrimidine, aromatic ketone, boron, sulfone, oxadiazole, triazole, thiazole, oxazole, and imidazole. Recently, several modifications have been done on both acceptor and donor moieties to enhance EL performances. Correspondingly, the maximum EQE of pure green TADF emitters reached almost 40%, and such accomplishment is possible when the suitable donor and acceptor moieties are incorporated in a way that can maintain the emission wavelength while retaining high efficiencies.[23–32]

Using D–A and D–A–D types of molecular design, green OLED devices achieved high EL performance with proper emission (Fig. 1). However, these types of emitters disclosed wide emission spectra, manifested as FWHM over 45 nm due to the strong ICT characteristics of the D–A skeleton. To satisfy the demands required by the international telecommunication union for the application of primary colors in ultra-high-definition displays, high color purity emitters possessing narrow full width at half maximum (FWHM) are required.[33–35] In 2016, Hatakeyama *et al.* proposed a new type of boron based

Yu-Jin Kim

Ms Yu-Jin Kim obtained her bachelor's degree in Chemical Engineering from Wonkwang University, Republic of Korea (2021 Aug). Currently, she is pursuing her master's degree in Chemical Engineering under the supervision of Prof. Bo-Mi Kim at Wonkwang University. Her research interests include the development of host and TADF materials for OLED applications.

Bo-Mi Kim

Prof. Bo-Mi Kim is an assistant professor at the department of Chemical Engineering, Wonkwang University, Republic of Korea. She received her PhD degree in Chemistry under the supervision of Prof. Kyu Yun Chai from Wonkwang University in 2014. Her research interests are the development of organic materials for OLED devices and bio-active applications.

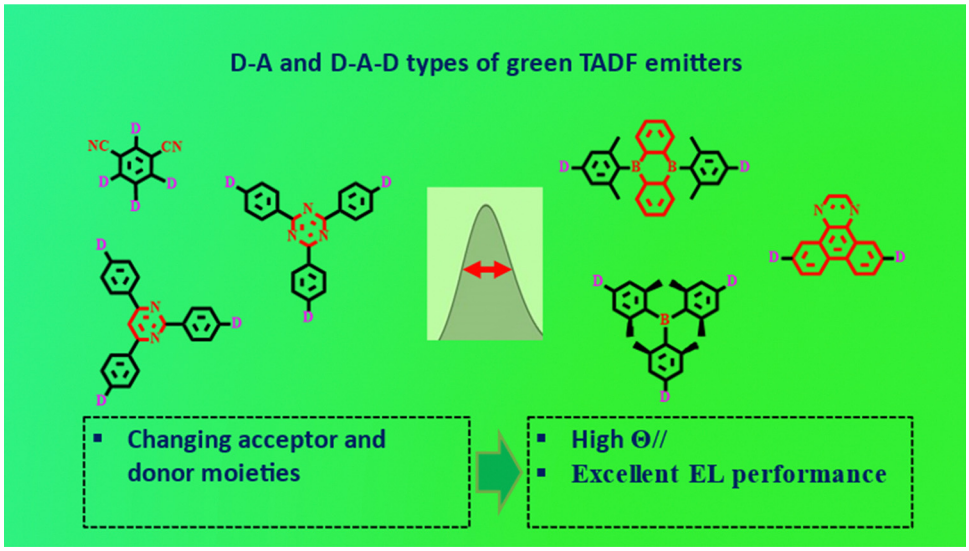

Fig. 1 Schematic illustration of acceptor moieties in conventional TADF emitters.

(DABNA) ultra-pure blue emitters for application in pure OLEDs. Unlike conventional TADF emitters, DABNA type emitters showed multi resonance properties through the alternative FMO distribution on different atoms, and these types of emitters are named as MR-TADF emitters. These types of emitters can reduce the FWHM (below 40 nm) *via* suppressing vibration and structural relaxation in the excited states.[36,37] After this breakthrough, several boron-based emitters were developed to obtain pure blue and sky-blue emissions. However, the development of pure green MR-TADF emitters is hindered at the early stage owing to a minimal understanding of the MR molecular framework. In recent years, the advancement of pure green MR-TADF emitters using boron and nitrogen-based BN core brought a positive impact on future display technologies. Anyhow, the progress of pure green emitters needs to hurry up to fulfill the necessity of the display market. This review is not intended to be an all-comprehensive summary of reported third generation green emitters (PL emission between 490–551 nm), but the intention is to offer a brief overview of the material design strategy of highly structured TADF and MR-TADF emitters with the aspect of emission wavelength, device performances, and color purity.

Green conventional TADF emitters

Cyano and triazine acceptor based green TADF emitters

In 2012, Adachi *et al.* developed cyano acceptor based **4CzIPN** emitter using multiple carbazole donors. Substituting multiple units on the phenyl ring tends to separate the FMOs and achieves a small ΔE_{ST} of 0.08 eV with an emission wavelength of 507 nm.[23] The external quantum efficiency (EQE) of the device was 19.3%. Further, several studies were conducted in different device configurations; interestingly, the EQE of the **4CzIPN** based device was improved to 31.2% by Lee *et al.* using a bipolar host material of **3CzPFP** in the emission layer.[24] The above emitter design guided the development of a series of cyano acceptor based TADF emitters, such as ***m*-4CzIPN**, **t-4CzIPN**, and **3DPA3CN**, for green OLED applications.[25,26] But the device performances were not satisfactory in terms of efficiencies (Fig. 1, 2 and Tables 1, 2).

Parallel to the development of cyano based green TADF emitters, heterocyclic triazine acceptor-based design accentuated the researchers engaged in TADF studies. The first triazine based pure green emitter surpassing electroluminescence (EL) emission over 525 nm was reported by Adachi *et al.*, and the emitter **PXZ-TRZ** based device revealed an EQE of 12.5%.[27] Acridine donor and triazine acceptor-based emitter **DMAC-TRZ** exhibited excellent EQE of 26.5%, but the emission was limited to the blueish-green region.[28] For application in solution processable green OLEDs, tri acridine donor and triazine based **3ACR-TRZ** emitter was reported by Kaji *et al.* (EQE-18.6%) with a bathochromic shifted emission compared to that of **DMAC-TRZ**.[29] The first donor–acceptor (D–A) type of green TADF emitter (**DACT-II**) achieving excellent device performance was reported in 2015 by Adachi *et al.* The emitter exhibited almost 100% PLQY, along with an extremely small ΔE_{ST} of 0.009 eV. Long conjugated emitter **DACT-II** exhibited a high horizontal dipole (Θ//) ratio of 86%. The EL emission of the TADF device was 525 nm, and the maximum EQE reached 29.6% without any outcoupling technique. Such achievement is supported by high PLQY, horizontal dipole ratio, and good TADF properties.[30] In 2019, our group developed a green TADF emitter **TRZ-DDPAc** using a diphenyl acridine donor and triazine acceptor in donor–acceptor–donor (D–A–D) molecular configuration. The emitter exhibited a small ΔE_{ST} of 0.03 eV and good TADF characteristics. The EL device showed emission of 525 nm and maximum EQE of 27.3%.[31]

In 2020, Liao *et al.* designed two green emitters **2tDMG** and **3tDMG** using face to face alignment of donor and triazine acceptor to activate the intramolecular non-covalent interaction. Both emitters revealed small ΔE_{ST} (<0.03 eV) and high PLQYs. Moreover, TADF properties of the emitters were good

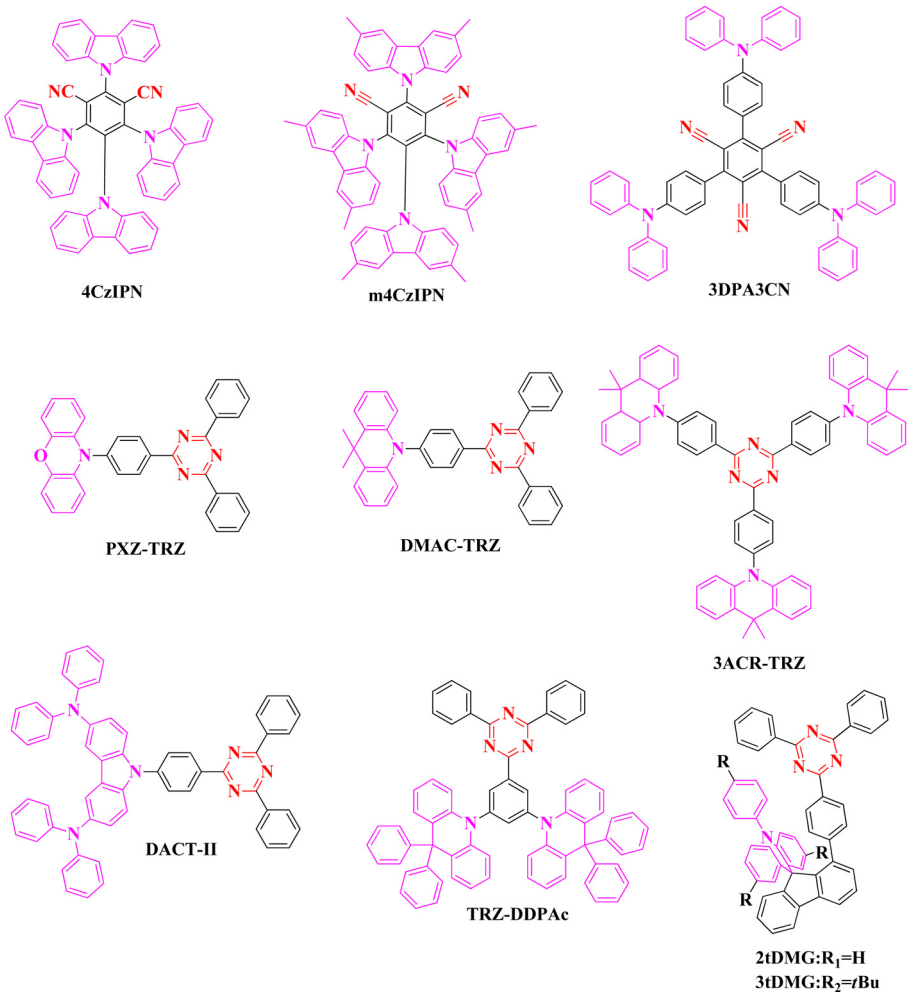

Fig. 2 Molecular structures of cyano and triazine acceptor based green TADF emitters.

with the support of a fast reverse intersystem crossing rate. The maximum EQE of **2tDMG** and **3tDMG** based devices were recorded as 30.8 and 26.3%, and the EL emissions were 504 and 518 nm, respectively. From the EL performances, it is understandable that non-covalent alignment design of D–A type emitters showed flat efficiency roll-off characteristics.[32]

Other acceptor-based green TADF emitters possessing high EL performances

Although the green TADF molecular design looks uncomplicated, surpassing EQE by over 30% using cyano and triazine based acceptors became a challenging part in the development process. Generally, EQE depends on IQE and light outcoupling efficiency; however, the out-coupling efficiency is limited to 20% in basic OLED devices. But the emitters demonstrate high horizontal dipole orientation, which has been proven to boost light out coupling efficiency in an effective manner, so it facilitates reinforcing the EL performance of the devices.

Lee *et al.* reported two green TADF emitters, **Pm2** and **Pm5**, using cyano substituted pyrimidine acceptors and acridine donors. Compared to the triazine, pyrimidine moiety has a slightly weaker electron accepting nature, and substituting the cyano group helped to maintain proper LUMO energy level (band gap). Both emitters revealed a high PLQY of over 95%, and a high reverse intersystem crossing rate of the order of 10^5 S^{-1}. Although the orientation ratio (60–66%) of both emitters was low, the EQE values were 31.3 and 30.6% for **Pm2** and **Pm5** based devices, respectively (Fig. 3 and Tables 3, 4). Surpassing EQE over 30% was supported by high PLQY and fast reverse intersystem crossing rate. This design revealed that triazine acceptor is not the only acceptor for designing green D–A type emitters, but various acceptor moieties with certain modifications also can be used.[38]

Another weak acceptor of two boron based green emitters was reported by Cheng *et al.* in 2018 by extending the horizontal ratio with D–A–D molecular skeleton. Two emitters, **CzDBA** and ***t*BuCzDBA**, showed PLQY of 100 and 86% and smaller ΔE_{ST} of 0.03 and 0.02 eV, respectively. Although the LUMO energy level of both the emitters (3.4 eV) was the same, the HOMO energy levels were different due to the attachment of *tert* butyl group on the carbazole donors of ***t*BuCzDBA**. Moreover, both emitters revealed high horizontal orientation of 84 and 83%, and with the support of the above parameters, the maximum EQEs were 37.8 and 32.4%, respectively. The EL emission

Table 1 Photophysical parameters of cyano and triazine based green TADF emitters

Emitter	PL (nm)	PLQY (%)	HOMO (eV)	LUMO (eV)	ΔE_{ST} (eV)	K_{RISC}	τ_d (μs)	Ref.
4CzIPN	507[a]	93.8[a]	5.80	3.40	0.08[a]	—	5.1	23 and 24
m-4CzIPN	—	67	—	—	0.01	—	2.6	25
t-4CzIPN	—	78	—	—	0.05	—	3.2	25
3DPA3CN	506[a]	82[a]	—	—	0.01[b]	2.0×10^{3}[b]	550	26
PXZ-TRZ	545[a]	65.7[b]	5.50	3.10	0.03[b]	—	0.68	27
DMAC-TRZ	500[b]	83[b]	5.30	2.78	0.05[b]	—	3.6	28
3ACR-TRZ	—	98[b]	—	—	0.01[a]	—	6.7	29
DACT-II	520[a]	100[b]	5.50	3.20	0.009[b]	6.8×10^{4}[b]	—	30
TRZ-DDPAc	511[a]	79.7[b]	5.72	2.87	0.03[b]	—	10.3	31
2tDMG	502[a]	87[b]	5.12	2.37	0.03[a]	2.2×10^{5}[b]	3.4	32
3tDMG	505[a]	86[b]	5.03	2.37	0.01[a]	3.2×10^{5}[b]	2.2	32

[a] Measured in solvent. [b] Measured in film.

Table 2 Device performances of cyano and triazine based green TADF emitters

Emitter	EL (nm)	CE (cd A^{-1})	PE (lm W^{-1})	EQE (%)	Host	Ref.
4CzIPN	—	—	—	31.2	3CzPFP	23 and 24
***m*-4CzIPN**	—	—	57.1	19.6	SiCz	25
t-4CzIPN	—	—	45.0	17.1	SiCz	25
3DPA3CN	—	—	—	21.4	DPEPO	26
PXZ-TRZ	529	—	—	12.5	CBP	27
DMAC-TRZ	—	66.8	65.6	26.5	mCPCN	28
3ACR-TRZ	—	36.3	—	18.6	CBP	29
DACT-II	525	—	—	29.6	CBP	30
TRZ-DDPAc	525	62.8	56.3	27.3	—	31
2tDMG	504	88.5	71.8	30.8	—	32
3tDMG	518	85.0	73.9	26.3	—	32

wavelength of **CzDBA** was 528 nm, while of ***t*BuCzDBA** was much red shifted to 542 nm, which was due to the narrow optical band gap.[39]

Expansion of the acceptor plane to adjust the molecular orientation of the green emitters, **PXZPM**, **PXZPyPM**, and **PXZTAZPM** was reported by Yang *et al.* in 2020. Pyrimidine based **PXZPM**, pyrimidine-pyridine based **PXZPyPM**, and triazine based **PXZTAZPM** emitters exhibited high PLQY of 100, 100, and 93%, respectively. All three emitters showed a good radiative rate of the order of 10^7 S^{-1}, and expansion of the acceptor plane using different acceptor moieties did not impact much on the photophysical and electrochemical properties. But the horizontal dipole ratios were 73, 84, and 86% for **PXZPM**, **PXZPyPM**, and **PXZTAZPM**, and the ratio was enhanced with the acceptor plane expansion. As a result, the maximum EQEs were 29.5, 33.9, and 30.1, with the EL emission wavelength of 528 nm. This study showed how it is possible to obtain high efficiencies by modulating the acceptor moieties and molecular plane.[40]

In 2021, Duan *et al.* reported a linear D–A–D type of diphenylamino carbazole and dibenzo quinoxaline based green emitter **DQBC**. Linear type of **DQBC** emitter showed excellent horizontal dipole orientation of 92%, and the EQE of the device was 39.1% with an EL emission of 534 nm. Achieving excellent EL performance not only depends on the orientation factor but is also supported by its high PLQY of 95% and fast reverse intersystem crossing rate of 1.1×10^6 S^{-1}. This is the highest EQE value ever reported for pure green TADF emitters so far.[41] This study proves that the selection of a suitable acceptor moiety and linear molecular arrangement leads to achieving proper emission wavelength and high device performance. Recently, Yang *et al.* reported star shaped D–A type of emitter **3DMAC-TB** with the combination of multiple acridine donors and triaryl boron acceptor. Steric hindrance between the peripheral donors and central triaryl boron made well separated HOMO and LUMO, which resulted in a small ΔE_{ST} of 0.03 eV. Consequently, a fast reverse intersystem crossing rate of 1.3×10^6 S^{-1} was calculated. Further, star shaped sterically hindered nature of **3DMAC-TB** emitter revealed a horizontal orientation ratio of 86%, which is comparable to the linear molecular skeleton-based emitters. The EQE value was 38.8% with the emission maxima of 508 nm, and enhanced EL performance conveys that star shaped molecules also can support a high horizontal orientation ratio.[42] However, color purity (narrow FWHM) cannot be controlled in D–A and D–A–D types of molecular skeletons due to their enhanced charge transfer characteristics and separated frontier molecular orbital distribution.

Green MR-TADF emitters

Since 2016, MR-TADF emitter-based research studies have expanded due to their fascinating properties, such as narrow FWHM and high PLQY. Blue emitting BN core with certain modifications exhibited considerable bathochromic shift. So, researchers put an effort to modify the BN core by substituting various acceptor or donor or both moieties on the main BN core or the peripheral region of carbazole units (Fig. 4). This part is

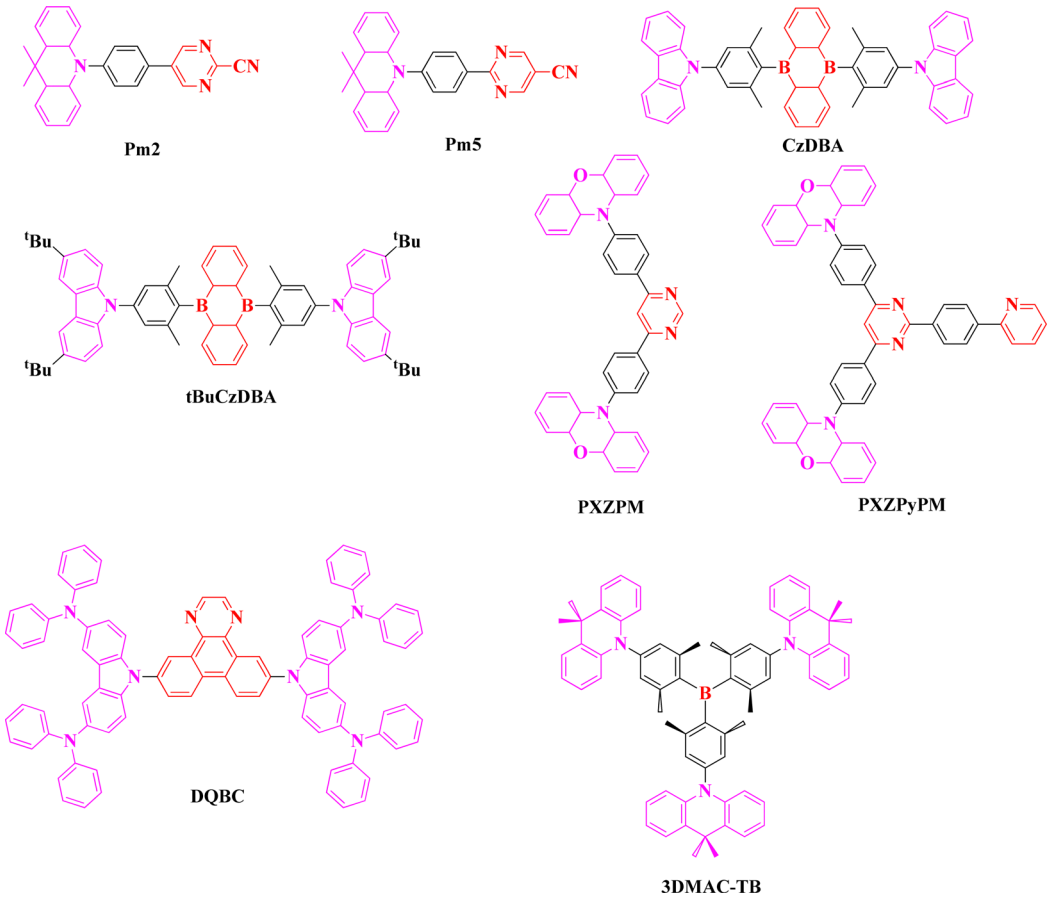

Fig. 3 Molecular structures of other acceptor based green TADF emitters.

Table 3 Photophysical and electrochemical summary of other acceptor-based green TADF emitters

Emitter	PL (nm)	PLQY (%)	HOMO (eV)	LUMO (eV)	ΔE_{ST} (eV)	K_{RISC}	τ_d (μs)	Ref.
Pm2	524[a]	100[b]	5.64	3.20	0.09[b]	1.5×10^{5}[b]	11.6	38
Pm5	543[a]	95[b]	5.63	3.22	0.04[b]	3.3×10^{5}[b]	5.2	38
CzDBA	524[b]	100[b]	5.93	3.45	0.033[b]	3.1×10^{5}[b]	3.2	39
***t*BuCzDBA**	553[b]	86[b]	5.88	3.49	0.022[b]	3.5×10^{5}[b]	2.1	39
PXZPM	525[b]	100[b]	5.10	2.42	0.04[b]	6.0×10^{5}[b]	2.98	40
RXZPyPM	524[b]	100[b]	5.08	2.36	0.07[b]	5.5×10^{5}[b]	2.41	40
PXZTAZPM	528[b]	93[b]	5.10	2.44	0.05[b]	5.4×10^{5}[b]	2.43	40
DQBC	551[a]	95[b]	5.07	2.68	0.06[a]	1.1×10^{6}[b]	5.5	41
3DMAC-TB	495[a]	94[b]	5.29	2.42	0.03[b]	1.3×10^{6}[b]	2.0	42

[a] Measured in solvent. [b] Measured in film.

Table 4 Device performance of other acceptor-based green TADF emitters

Emitter	EL (nm)	CE (cd A^{-1})	PE (lm W^{-1})	EQE (%)	Θ// (%)	Ref.
Pm2	530	104.5	117.2	31.3	66	38
Pm5	535	103.7	116.3	30.6	60	38
CzDBA	528	139.6	121.6	37.8	84	39
***t*BuCzDBA**	542	127.9	109.8	32.4	83	39
PXZPM	528	98.4	103.5	29.5	73	40
RXZPyPM	528	113.5	118.9	33.9	84	40
PXZTAZPM	528	101.3	106.1	30.1	86	40
DQBC	534		112.0	39.1	92	41
3DMAC-TB	508	111.9	109.6	38.8	86	42

divided into several sections based on molecular design strategy, which will help an easy understanding of green MR-TADF emitters.

(a) Acceptor attachment on BN core

In 2019, Duan *et al.* proposed a strategy to develop bathochromic shifted emission by modifying the parent DABNA core. Here, they have amplified the skeleton while extending the peripheral region with a fluorobenzene substitution at the *para* position of the B atom. Three emitters, **2F-BN**, **3F-BN**, and **4F-BN** were designed and synthesized through a one pot borylation reaction. From the calculation evidence, it was noticed that the

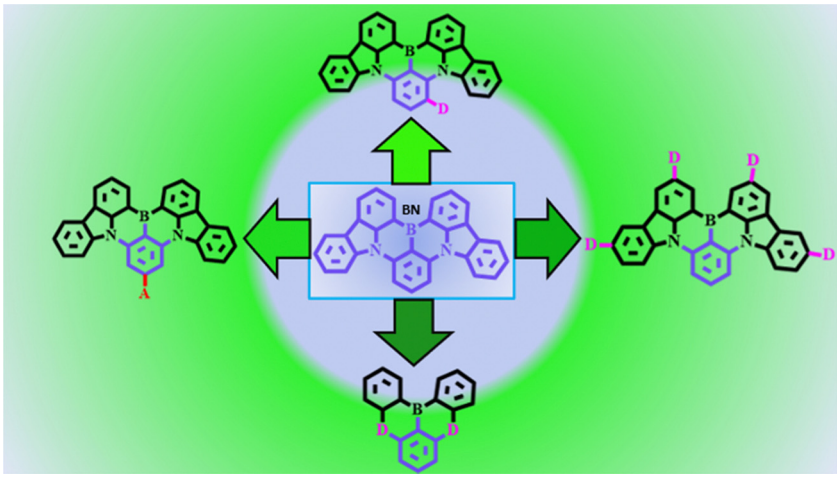

Fig. 4 Schematic illustration of green MR-TADF emitters modified from BN core.

extension of LUMO distribution up to the peripheral region tends to reduce the band gap, which supported a bathochromic shifted emission of 494, 499, and 496 nm for **2F-BN**, **3F-BN**, and **4F-BN**, respectively (Fig. 5 and Tables 5, 6). The electroluminescence (EL) performance of three emitters was studied, and the EL emission and FWHM were 501/40, 499/38.5, 493/31.6 nm, and the maximum external quantum efficiency values (EQE) of devices were 22, 22.7 and 20.9% for **2F-BN**, **3F-BN**, and **4F-BN** based devices, respectively. Such device performance was much better than that of conventional green TADF emitter of **4CzIPN** in terms of color purity and efficiency in a similar device structure. This study initiated an eye-opening path for designing bathochromic shifted emission materials, especially green MR-TADF emitters.[43]

The same group in 2020 developed an Aza fused green MR-TADF emitter using modification on BN core (**AZA-BN**). This study brought an interesting theme in both chemistry and MR-TADF emitters. Aza fused emitter was synthesized using the imino nitrogen centered radical-based cyclization. The calculation results indicated the Aza fused ring on BN core effect in both HOMO and LUMO distribution, which was not observed in the previous design of **2F-BN** emitter. Phosphorescence sensitized devices were fabricated, and EL emission was in the pure green region (527 nm) with a maximum EQE of 28.2%. Extended conjugation and fused Aza skeleton showed improvement in color purity as well as PLQY value.[44]

In 2021, Wang *et al.* continued the development of green MR-TADF emitters by attaching strong electron withdrawing groups at the *para* position of the B atom in BN core. Four emitters, **DtCzB-DPTRZ**, **DtCzB-TPTRZ**, **DtCzB-PPm**, and **DtCzB-CNPm** were designed by attaching triazine, phenyltriazine, pyrimidine, and pyrimidine-cyano moieties, respectively. Such attachment at the *para* position depressed the LUMO energy level, which helped to decrease the band gap, and the photoluminescence (PL) emissions were between 499–521 nm. At the same time, **DtCzB-TPTRZ** emitters exhibited a high PLQY of 97%. As a result, **DtCzB-TPTRZ** based TADF devices showed good efficiency enhancement (EQE of 29.8%) with EL maxima of 516 nm. To achieve more efficiency and less roll-off, **5tBuCzBN** assistant dopant based hyperfluorescence device using **DtCzB-TPTRZ** as the final emitter was fabricated, and the device EQE surpassed 30% while showing the emission at 520 nm.[45]

(b) Multiple donor attachment on BN core

In 2020, the first green emitter based on auxiliary donor attachment to the BN core was reported by Wang *et al.* The emitter ***m*-Cz-BNCz** showed both twisted donor–acceptor and multi resonance characteristics. Attaching the carbazole derivative at the *meta* position to the B atom increased the HOMO energy level, which helped to red shift the emission compared to the parent BN core. The PL emission was noticed around 519 nm, and the PLQY in the solution state was as high as 97%. Moreover, a low ΔE_{ST} of 0.08 eV supported good TADF properties as well, and reverse intersystem crossing rate was enhanced to 1.4×10^6 S^{-1}. The EL efficiencies of the green device (EL emission-528 nm; EQE-31.4%) was better than that of acceptor-BN core based green emitters, but the FWHM was wider (45 nm) due to its good charge transfer characteristics.[46]

Further study on donor attachment with BN core was continued by Yasuda *et al.*, and they reported a series of carbazole embedded polycyclic heteroaromatic based emitters, where attaching multiple carbazole units at the *ortho*, *meta*, and *para* positions of B atom brought different approaches on bathochromic shifted emission. Five carbazoles attached **BBCz-G** emitter revealed PL emission of 517 nm and FWHM of 34 nm along with high reverse intersystem crossing rate constant in the order of 10^5 S^{-1}. The device performance of **BBCz-G** based green device (515 nm) showed a maximum EQE of 31.8%, but the FWHM of the device was broadened to 54 nm due to the planar molecular skeleton. Further investigation on bathochromic shifted emissions using the BN core was carried out in 2021 by the same group. Unlike the previous design, additional carbazole moieties were capped at the 3rd and 6th positions of BN carbazole moiety (**TCz-B**). Just increasing the donor strength of BN core and its effect on HOMO distribution

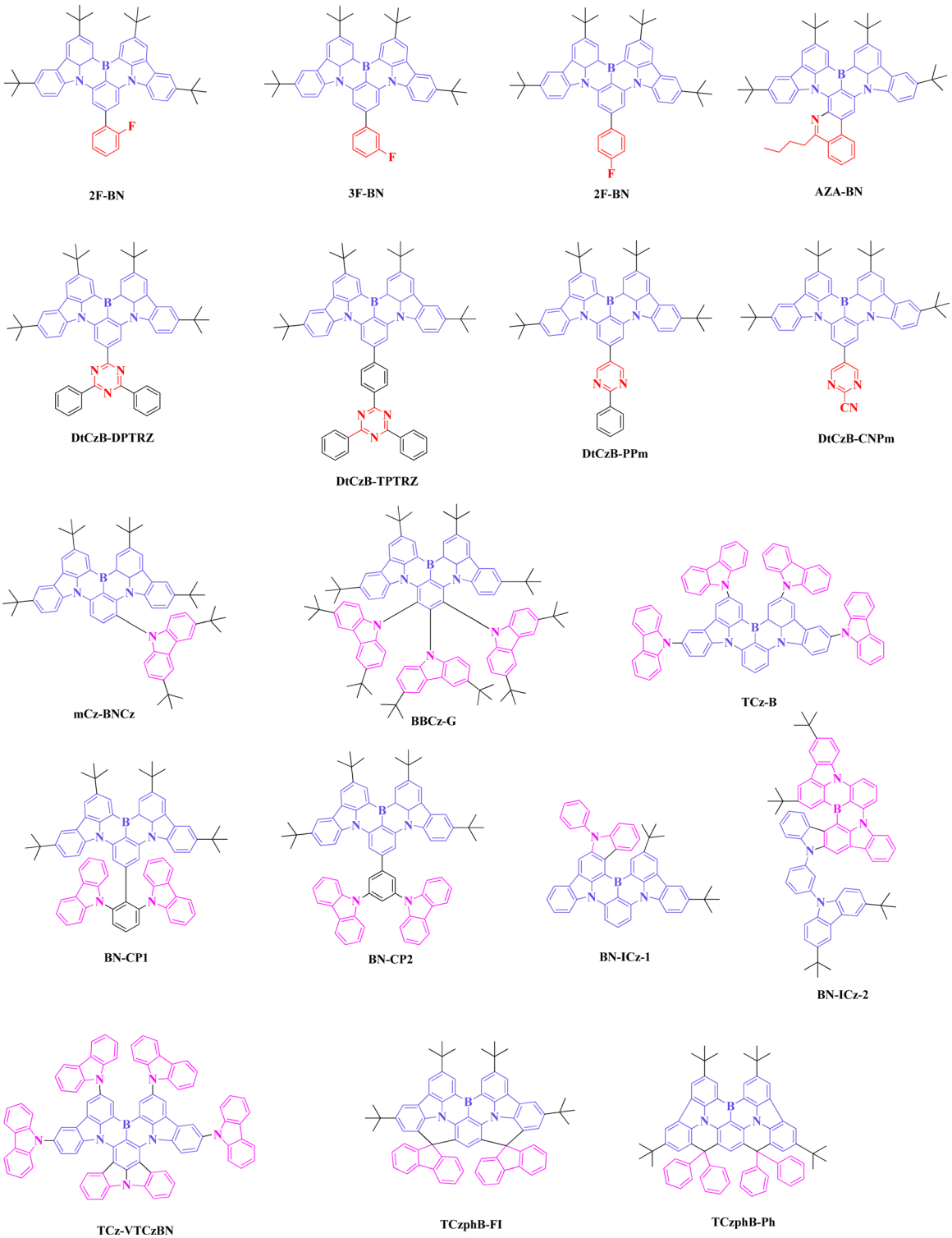

Fig. 5 Green MR-TADF molecular structures based on acceptor and multiple donors' attachment on BN core.

tend to show bathochromic shifted emission of 512 nm, and which is comparably a large shift from the parent BN core (477 nm-**Cz-B**). This design concept did not show much effect on FWHM broadening (solution FWHM-27; device FWHM-30 nm), and the EQE was 29.2% with a green emission of 515 nm.[47,48]

Achieving high device performance and maintaining good efficiencies at high doping concentration was identified as a big hurdle in BN core-based emitters due to its planar skeleton. In 2021, Yang *et al.* proposed quenching resistance emitters by attaching bulky carbazole donor derivatives on BN core, **BN-CP1** and **BN-CP2.** Attaching such donor moieties at 1 and 3rd positions

Table 5 Photophysical and electrochemical properties of MR-TADF green emitters

Emitter	PL (nm)	PLQY (%)	HOMO (eV)	LUMO (eV)	S_1 (eV)	T_1 (eV)	ΔE_{ST} (eV)	K_{RISC}	Ref.
2F-BN	494[a]	88.7[b]	5.16	2.65	2.51[a]	2.35[a]	0.16[a]	2.2×10^{4}[b]	43
3F-BN	499[a]	83.4[b]	5.09	2.60	2.48[a]	2.40[a]	0.08[a]	3.9×10^{4}[b]	43
4F-BN	496[a]	91.4[b]	5.10	2.60	2.50[a]	2.39[a]	0.11[a]	4.4×10^{4}[b]	43
AZA-BN	522[a]	94.0[b]	5.07	2.73	2.37[a]	2.19[a]	0.18[a]	7.5×10^{3}[b]	44
DtCzB-DPTRZ	521[a]	94[a]	5.30	2.99	2.33[a]	2.15[a]	0.18[a]	0.1×10^{4}[b]	45
DtCzB-TPTRZ	501[a]	97[a]	5.37	2.82	2.44[a]	2.33[a]	0.11[a]	1.1×10^{4}[b]	45
DtCzB-PPm	499[a]	96[a]	5.40	2.75	2.43[a]	2.32[a]	0.11[a]	1.0×10^{4}[b]	45
DtCzB-CNPm	515[a]	93[a]	5.47	2.96	2.28[a]	2.13[a]	0.15[a]	0.1×10^{4}[b]	45
***m*-Cz-BNCz**	519[a]	97[a]	5.15	2.63	—	—	0.08[a]	1.4×10^{6}[b]	46
BBCz-G	517[a]	90[a]	5.70	3.20	2.50[a]	2.36[a]	0.14[a]	1.8×10^{5}[a]	47
TCz-B	512[a]	100[a]	—	—	2.42[a]	2.33[a]	0.99[a]	2.0×10^{4}[a]	48
BN-CP1	490[a]	93[b]	4.91	1.71	—	—	0.12[a]	1.5×10^{4}[b]	49
BN-CP2	490[a]	91[b]	5.13	1.88	—	—	0.13[a]	1.4×10^{4}[b]	49
BNICz-1	521[a]	99.2[a]	5.62	3.25	2.38[a]	2.16[a]	0.22[a]	2.9×10^{4}[a]	50
BNICz-2	520[a]	98.3[a]	5.20	2.78	2.38[a]	2.20[a]	0.18[a]	6.4×10^{4}[a]	50
TCz-VTCzBN	521[a]	98[a]	5.28	2.98	2.49[a]	2.49[a]	<0.01[a]	0.9×10^{6}[a]	51
tCzphB-Ph	523[a]	98[a]	5.15	2.72	—	—	0.04[a]	—	52
tCzphB-Fl	531[a]	93[a]	5.12	2.73	—	—	0.04[a]	—	52
TRZCzPh-BNCz	514[a]	93[a]	5.43	3.01	2.48[a]	2.35[a]	0.13[a]	2.1×10^{6}[a]	53
TRZTPh-BNCz	513[a]	94.7[a]	5.36	2.95	2.49[a]	2.38[a]	0.11[a]	1.6×10^{6}[a]	53
PXZ-BN	502[a]	90[b]	—	—	—	—	0.17[a]	0.9×10^{4}[b]	54
TPXZBN	502[a]	91[a]	5.08	2.54	—	—	0.16[a]	0.5×10^{5}[b]	55
DPXZCZBN	500[a]	90[a]	5.25	2.69	—	—	0.13[a]	1.1×10^{5}[b]	55
2PTZBN	510[a]	80[b]	5.19	2.73	2.59[a]	2.44[a]	0.15[a]	2.8×10^{5}[a]	56
Cz-PTZ-BN	510[a]	91	5.38	2.86	2.57[a]	2.46[a]	0.11[a]	0.8×10^{5}[a]	57
2Cz-PTZ-BN	505[a]	96	5.35	2.83	2.59[a]	2.50[a]	0.09[a]	1.0×10^{5}[a]	57
(***P*/*M*-helicene-BN**	520[a]	98[a]	—	—	—	—	0.15[b]	4.6×10^{4}[b]	58
BN-MeIAc	497[a]	96[b]	5.30	2.80	—	—	0.11[a]	6.3×10^{4}[b]	59
OAB-ABP-1	506[b]	90.0[b]	—	—	—	—	0.12[b]	4.0×10^{4}[b]	60
ν-DABNA-CN-Me	496[a]	86[a]	5.80	3.40	—	—	0.12[a]	1.6×10^{5}[a]	61
***p*-DiNBO**	500[a]	96[b]	5.40	3.00	2.54[a]	2.48[a]	0.06[a]	1.4×10^{4}[b]	62
DDiKTa	490[b]	—	—	—	—	—	0.16[b]	—	63
QAD-2Cz	506[a]	99.5[b]	5.87	3.58	—	—	0.17[a]	—	64

[a] Measured in solvent. [b] Measured in film.

of the extended phenyl ring, enabling steric hindrance, helped to reduce the detrimental excimers. But these two emitters exhibited large ΔE_{ST} of around 0.12 eV and lower reverse intersystem crossing rate. So, it can be noted that the charge transfer characteristics of both emitters are mitigated by attaching the donor moieties to the extended phenyl ring. As a result, FWHM of the devices was narrowed (25 nm), but the emission color was around 496 nm, which was not in the pure green region. The maximum EQE of **BN-CP1** based device was 40%, and the EQE remained at 33.3% even at a high (30 wt%) doping concentration. It can be noted that such a design strategy led to reducing the quenching while enhancing the device performances.[49]

An interesting design of utilizing rigid indolocarbazole and carbazole derivatives based pure green emitters was reported by Duan *et al.* Two emitters, **BNICz-1** and **BNICz-2** exhibited high PLQY over 98% and FWHM of 21 nm. The EL performance of the devices was quite similar to each other, and the EL_{max} emissions were observed at 523 nm. The maxima of EQE reached 30.5% along with a narrower FWHM of 23 nm while maintaining the pure green emission (CIE *x*, *y*: 0.17, 0.78). The rigid, extended conjugation, reduced vibrational frequencies, and horizontal orientation factor of over 79% helped to obtain superior performance in pure green devices.[50]

Although the emission wavelength and efficiencies were improved, the efficiency roll-off characters were not alleviated. Recently, in 2022, Zuo *et al.* designed a green emitter (**TCz-VTCzBN**) by fused hybridization of the above **TCz-B** green emitter and violet emitting **tDIDCz**. Due to the extension of delocalization through peripheral carbazole donor moieties, an extremely pure green PL emission of 521 nm with a FWHM of 29 nm was obtained. This fused hybridized design strategy helped to enhance the reverse intersystem crossing rate constant up to 10^6 S^{-1} through large spin orbital coupling (SOC) and a low ΔE_{ST} value below 0.01 eV. Symmetrical molecular skeleton improved the horizontal dipole ratio. With the help of a high PLQY (98%) and horizontal ratio of 94%, the green device was able to achieve a high EQE of 32.2% with an emission wavelength of 524 nm. Although the efficiency values were high, the color purity was not satisfactory due to its wider FWHM of 37 nm.[48,51]

To gratify the color purity while maintaining the device performances, Zhang *et al.* reported two pure green emitters, **tCzphB-Ph** and **tCzphB-Fi**, using a locking strategy between the outer phenyl ring of carbazole and the central phenyl ring with diphenyl fluorene and rigid spiro fluorene skeletons. This locking strategy on BN core effectively suppressed the distortion and vibration modes in the excited state. The EL properties of **tCzphB-Ph** based bottom emission devices were 29.3% of EQE and EL emission of 527 nm along with narrower FWHM of 24 nm. This is the narrowest FWHM reported for any green

Table 6 Device performances of MR-TADF green emitters

Emitter	EL (nm)	CE (cd A^{-1})	PE (lm W^{-1})	EQE	FWHM	Ref.
2F-BN	501	—	69.8	22.0	40	43
3F-BN	499	—	72.3	22.7	38	43
4F-BN	493	—	51.3	20.9	31	43
AZA-BN	527	—	121.7	28.2	30	44
DtCzB-DPTRZ	532	88.6	92.7	24.6	39	45
DtCzB-TPTRZ	516	93.2	98.8	29.8	38	45
DtCzB-PPm	508	87.5	92.1	28.6	33	45
DtCzB-CNPm	540	99.1	107.4	25.0	44	45
***m*-Cz-BNCz**	528	117.6	127.4	31.4	45	46
BBCz-G	515			31.8	54	47
TCz-B	515	100.7	72.4	29.2	30	48
BN-CP1	496	83.8	109.7	40.0	25	49
BN-CP2	497	82.6	108.1	36.4	26	49
BNICz-1	523	—	84.2	30.5	23	50
BNICz-2	523	—	102.9	29.8	23	50
TCz-VTCzBN	524	129.3	96.7	32.2	37	51
tCzphB-Ph	527	—	—	29.3	24	52
tCzphB-Fi	535	—	—	26.2	26	52
TRZCzPh-BNCz	513	—	101.4	32.5	37	53
TRZTPh-BNCz	513	—	99.5	31.4	33	53
PXZ-BN	516	—	—	23.3	47	54
TPXZBN	506	64.8	37.0	21.3	37	55
DPXZCZBN	505	61.6	43.2	19.2	36	55
2PTZBN	528	96.5	86.6	25.5	58	56
Cz-PTZ-BN	520	100.4	86.1	27.6	54	57
2Cz-PTZ-BN	516	108.5	92.1	32.8	56	57
(***P*-helicene-BN**	524	117.5	153.8	31.5	49	58
BN-MeIAc	504	103.0	130.2	37.2	33	59
OAB-ABP-1	505	53.2	45.3	21.8	33	60
ν-DABNA-CN-Me	504	89.0	137.6	32.0	23	61
***p*-DiNBO**	513	79.5	60.4	21.6	48	62
DDiKTa	500	52.4	44.4	19.0	59	63
QAD-2Cz	530	103.1	104.4	27.3	56	64

single boron-based MR-TADF emitters possessing a CIE y value near 0.77.[52]

(c) Donor and acceptor attachment on BN core

In 2022, You *et al.* proposed a new space confined donor–acceptor strategy using the BN core. Two emitters, namely **TRZCzPh-BNCz** and **TRZTPH-BNCz** were reported with carbazole-triazine and terphenyl-triazine attachment on BN core. Such donor–acceptor on the central phenyl atom of BN core induced intermediate triplet states and effectively enhanced the reverse intersystem crossing rate of both emitters over 1.55×10^6 S^{-1} with the help of multi-channel activation. This strategy brought a way of enhancing the rate of reverse inter system crossing without any heavy atom effect that led to achieving alleviated efficiency roll-off, as revealed in the device performance, the maximum EQE was high as 32.5% and maintained at 22.9% at 1000 cd m^{-2}. This is the highest EQE value for pure green MR-TADF based boron embedded emitters so far.[53]

(d) Heteroatom-donor based core

In 2021, Kido *et al.* reported a pure green MR-TADF emitter of **PXZ-BN** using a strong phenoxazine donor at the peripheral region. Compared to weak electron donating carbazole based blue emitting BN core, phenoxazine gave bathochromic emission over 500 nm without any other additional donor support (Fig. 6 and Tables 5, 6). The maximum EQE of 23.3% was recorded with the emission of 516 nm, but the FWHM was 10 nm wider (47 nm) compared to that of in solution state (38 nm). As a continuity work of phenoxazine donor based green MR-TADF emitter, Zheng *et al.* reported two emitters, **TPXZBN** and **DPXZCZBN** by attaching one more phenoxazine and tetra methyl carbazole at *para* positions, respectively. Tri phenoxazine substituted **TPXZBN** showed a slight bathochromic shifted emission of 502 nm, compared with the **DPXZCZBN** (500 nm) emitter due to the strong donor effect of phenoxazine at the *para* position to that of B atom that reduced the band gap *via* affecting the LUMO energy level. Such an effect is higher when a strong donor is attached to that position. The EL performances of **TPXZBN** were better than that of **DPXZCZBN**. The FWHM of both emitters was maintained at 36 nm, which is much better than the planar parent molecule of **PXZ-BN**.[54,55]

In 2021, Yang *et al.* proposed a design strategy of enhancing the reverse intersystem crossing rate of green MR-TADF emitters by substituting sulfur atom embedded phenothiazine based **2PTZBN** emitter, which has a similar molecular pattern to that of **PXZ-BN**. As an effect of a heavy sulfur atom, the reverse intersystem crossing rate of **2PTZBN** was 2.7 times higher than that of phenoxazine based **PXZ-BN**. The much stronger donor strength of phenothiazine led to bathochromic shifted emission in the case of **2PTZBN**. The EL emission was 528 nm, and the maximum EQE was 25.5%. From both device data, it can be observed that heavy atom based **2PTZBN** revealed better resistance to efficiency roll-off due to its fast flip rate.[56]

Since utilizing heteroatom donors in designing green MR-TADF emitters drew attention, Yang *et al.* in 2022 reported two asymmetric emitters, **Cz-PTZ-BN** and **2Cz-PTZ-BN** based on phenothiazine and carbazole derivatives. Both emitters revealed a small ΔE_{ST} and considerably higher reverse intersystem crossing rate (10^5 S^{-1}). The presence of heavy atoms in the BN core enhanced the reverse intersystem crossing rate *via* SOC. The device based on **2Cz-PTZ-BN** exhibited a maximum EQE of 32.8%, and the EL emission was 516 nm, along with a wide FWHM of 56 nm. Out of phenoxazine and phenothiazine donor based green emitters, this study brought much better EL performances, but the color purity was not achieved compared to only carbazole derivative based green MR-TADF emitters.[57]

(e) CPL based green MR-TADF emitters

In 2022, Yang *et al.* demonstrated a new type of circularly polarized chiral type of MR-TADF emitter containing boron, nitrogen, and sulfur, ***P*/*M*-helicene-BN**. It showed a high PLQY of nearly 100% and strong CPL characteristics. Sulfur embedded helicene based BN core exhibited pure green emission around 524 nm with FWHM of 49 nm and achieved a high EQE value of 31.5%, which has much better performance than other heteroatom-based MR-TADF emitters (Fig. 6 and Tables 5, 6). This study brought an approach of utilizing helicene based molecules in MR-TADF applications. The same group has reported chiral green emitters using acridan quaternary carbon stereocenter. The emitter (*R*/*S*)-**BN-MeIAc** exhibited a high PLQY

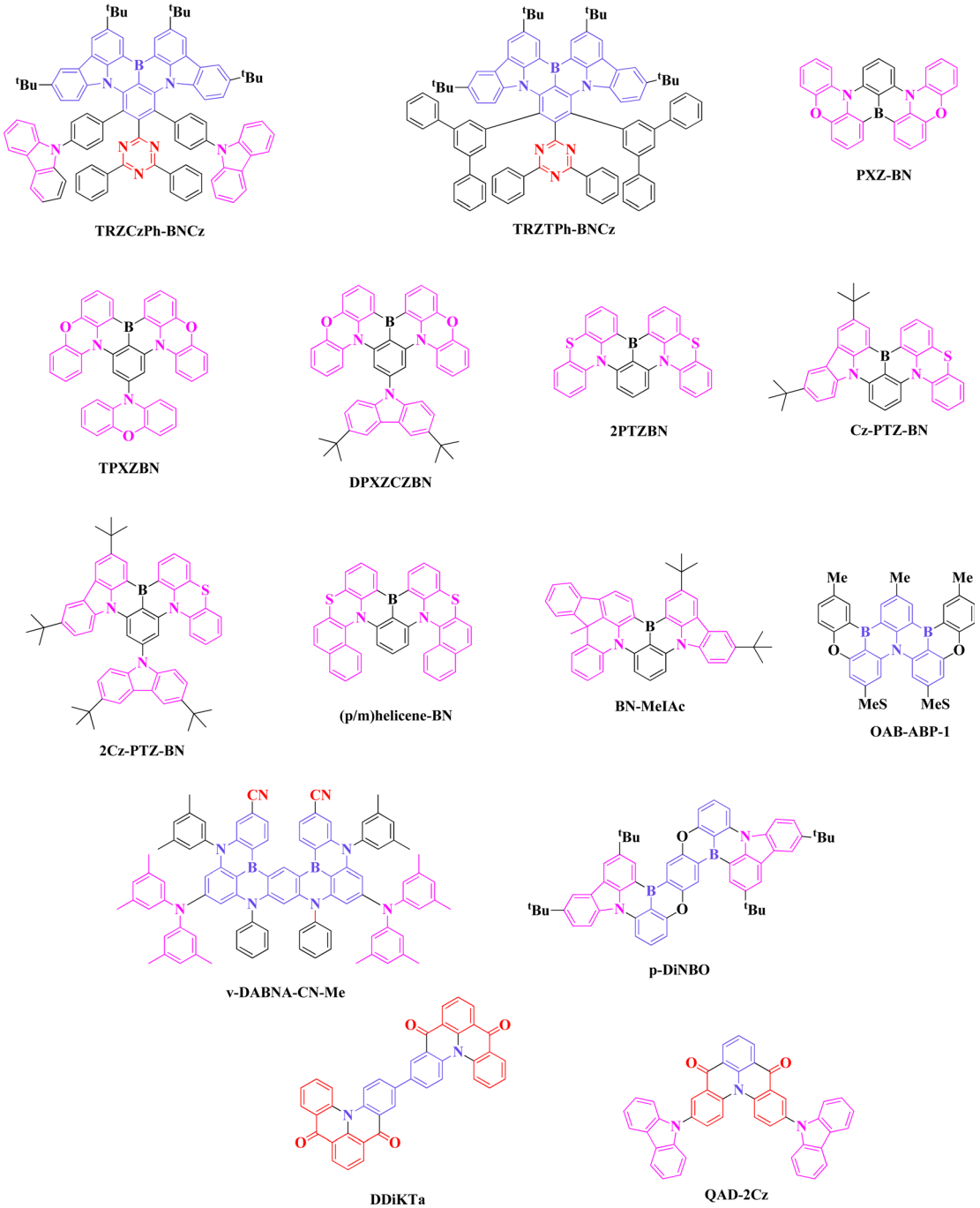

Fig. 6 Molecular structures of other green MR-TADF emitters.

of 96% and a singlet radiative rate of the order of 10^7 S^{-1}. The EL device using chiral emitter (*R*)-**BN-MeIAc** exhibited a maximum EQE of 37.2% with the support of PLQY and high horizontal orientation of 90%. The EL emission was 504 nm, along with a narrow FWHM of 33 nm, which is much better than the previous helicene based emitter. Although the color purity and efficiencies are better, the emission wavelength was blue shifted. This study opens a path for designing chiral emitters for CP-OLED applications with good EL performances.[58,59]

(f) Double boron core

In 2020, Hatakeyama *et al.* designed and synthesized an emitter **OAB-ABP-1** by combining the molecular skeletons of **DOBNA** and **ADBNA** emitters for application in solution processable devices (Fig. 6 and Tables 5, 6). To eliminate such undesired products during the synthesis and aggregation issues associated with device fabrication, mesityl groups were introduced at the *para* position to that of boron atoms. Double boron embedded emitter, **OAB-ABP-1**, revealed a narrow FWHM of

33 nm with an emission wavelength of 505 nm, and EQE of 21.8% in polymer-based solution processable device. Further, the device half-lifetime of 11 h at initial luminescence (300 cd m^{-2}) was recorded and is one of the best among solution processable TADF-OLEDs. This study brought an effective approach to designing pure green emitters for solution processable OLEDs, and the performances are comparable to that of thermal evaporation devices. Recently, the same group has designed a green emitter, **ν-DABNA-CN-Me** using modification of double boron embedded sky blue **ν-DABNA** emitter. Here, color shift towards 496 nm was achieved by attaching electron withdrawing cyano moieties at the *para* position of the boron atom. Compared to the previous double boron based green MR-TADF emitter **OAB-ABP-1**, **ν-DABNA-CN-Me** based device showed a much narrower FWHM of 23 nm at the same emission wavelength. With the support of high orientation and PLQY, the maximum EQE was 32.0% at a low doping concentration (0.5 wt%).[60,61]

Double boron, oxygen, and nitrogen embedded molecular structure of ***p*-DiNBO** was recently reported by Kido *et al.* Connecting two boron atoms through 1–4th position led to a bathochromic shift, but the shift was controlled near 500 nm by attaching weak and strong electron donating oxygen and nitrogen atoms. Further, extending the structure through dimerization helped to strengthen the horizontal molecular orientation up to 92%. The device using ***p*-DiNBO** as MR-TADF emitter revealed a maximum EQE of 21.6%, and the emission wavelength was 513 nm along with FWHM of 48 nm.[62]

(g) Amine and carbonyl-based core

In 2020, Colman *et al.* reported a boron free MR-TADF emitter, **DdiKTa**, for green device applications. This is a dimeric material, which consists of similar units of **DiKTa** emitter. **DDiKTa** skeleton is composed of amine and carbonyl units, which conserves its multi resonance characters even in dimeric form. EL performance in the polar host medium was reported, and it showed a maximum EQE of 19% with an emission wavelength of 500 nm (Fig. 6 and Tables 5, 6). Even though the Stokes shift and CT characters were smaller, the FWHM of the device was much wider at 59 nm. Another study on carbonyl and nitrogen based green MR-TADF emitters (**QAD-2Cz**) was reported in 2021 by Zhang *et al.* Attaching carbazole moieties on both sides of rigid QAD core brought green emission of 506 nm while retaining the multi resonance effect. Such color tuning was possible by adjusting the band gap while shifting the HOMO energy level through different donor moieties. The device revealed emission around 530 nm, and EQE was improved to 27.3%, but the FWHM of the device was 56 nm. Although the boron free green MR-TADF emitter-based device efficiencies and emission color were improved, unfortunately, color purity was not achieved, which may be due to the CT characteristics of the main core.

Summary and future perspective

In this review, a detailed summary of green TADF emitters based on the molecular design strategy is discussed. In the initial stage, green TADF emitters were constructed using cyano and triazine acceptor moieties and were able to reach 29% of EQE. Not limited to those two acceptor moieties, other acceptor moieties were also utilized in green TADF molecular design. But the progress of achieving high device performance was hampered compared to other primary colors. However, a few green TADF emitters bearing high horizontal molecular orientation have been reported, and their EL performances were potentially enhanced. In 2021, a green D–A–D type of TADF emitter revealed a competitive EQE value surpassing 39% with the help of an appropriate molecular design. Donor and acceptor based conventional green TADF emitters manifested satisfactory EL efficiencies; nevertheless, the color purity was not good enough to meet the need for next generation display technology.

In recent years, boron-based MR type of TADF emitters have made a chronicle of fluorescence emitters' history. In the early growth stage of MR-TADF emitters, it was difficult to make bathochromic shifted emissions, but several approaches are being conducted while making modifications to blue MR-TADF emitters. Recent reports indicate that the blue BN emitter is one of the essential cores utilized for bathochromic shifted emissions. Modifications are done using BN as the center core material and decoration is made around the peripheral and terminal regions, such as attaching the acceptor or donor or both moieties at the *para* and *meta* position to that of the boron atom, respectively. Simultaneously, other types of emitting cores are adapted to make bathochromic shifted emission, like attaching strong electron donors and multiple heteroatom donors adjacent to the boron atom. Further, the narrowing FWHM process is continued using the double boron embedded extended DABNA core, and considerable color purity (FWHM of 23 nm) was achieved while retaining the emission wavelength in the pure green region. The main concern about these (boron) types of emitters is associated with the synthetic yield and purification of the emitters. To overcome such issues, boron free MR-TADF emitters are introduced, but the performances are not satisfactory compared to the boron based green emitters in terms of color purity. So, further studies on green emitter design are required to get better color purity and easy synthesis. At the same time, there is no clear evidence related to the lifetime study of green MR-TADF emitters found in the reports, so further investigation related to lifetime should be done in order to satisfy future demands in display technology.

Author contributions

Conceptualization, R. B.; writing original draft, R. B.; methodology, R. B.; writing-review & editing, R. B.; visualization R. B. and K. R.; support writing, K. R. and Y. J. K.; funding acquisition, B.-M. K.

Conflicts of interest

There are no conflicts to declare towards this work.

Acknowledgements

This work is supported by Wonkwang University (Wonkwang University-2022). We dedicate this work to Professor. Kyu Yun Chai on the occasion of his happy retirement and wonderful career.

References

1 B. Geffroy, P. Le Roy and C. Prat, Organic light-emitting diode (OLED) technology: materials, devices and display technologies, *Polym. Int.*, 2006, **55**(6), 572–582.
2 Y. Sun, N. C. Giebink, H. Kanno, B. Ma, M. E. Thompson and S. R. Forrest, Management of singlet and triplet excitons for efficient white organic light-emitting devices, *Nature*, 2006, **440**(7086), 908–912.
3 G. Hong, X. Gan, C. Leonhardt, Z. Zhang, J. Seibert, J. M. Busch and S. Bräse, A brief history of OLEDs---emitter development and industry milestones, *Adv. Mater.*, 2021, **33**(9), 2005630.
4 C. Cebrián and M. Mauro, Recent advances in phosphorescent platinum complexes for organic light-emitting diodes, *Beilstein J. Org. Chem.*, 2018, **14**(1), 1459–1481.
5 G. E. Norby, C. D. Park, B. O'Brien, G. Li, L. Huang and J. Li, Efficient white OLEDs employing red, green, and blue tetradentate platinum phosphorescent emitters, *Org. Electron.*, 2016, **37**, 163–168.
6 B. Diouf, W. S. Jeon, R. Pode and J. H. Kwon, Efficiency control in iridium complex-based phosphorescent light-emitting diodes, *Adv. Mater. Sci. Eng.*, 2012, **2012**, 794674.
7 C. Ulbricht, B. Beyer, C. Friebe, A. Winter and U. S. Schubert, Recent developments in the application of phosphorescent iridium (III) complex systems, *Adv. Mater.*, 2009, **21**(44), 4418–4441.
8 X. Wu, M. Zhu, D. W. Bruce, W. Zhu and Y. Wang, An overview of phosphorescent metallomesogens based on platinum and iridium, *J. Mater. Chem. C*, 2018, **6**(37), 9848–9860.
9 A. R. Smith, P. L. Burn and B. J. Powell, Spin–Orbit Coupling in Phosphorescent Iridium (III) Complexes, *Chem. Phys. Chem.*, 2011, **12**(13), 2429–2438.
10 C. H. Yang, Y. M. Cheng, Y. Chi, C. J. Hsu, F. C. Fang, K. T. Wong and C. C. Wu, Blue-emitting heteroleptic iridium (III) complexes suitable for high-efficiency phosphorescent OLEDs, *Angew. Chem.*, 2007, **119**(14), 2470–2473.
11 M. Zhu and C. Yang, Blue fluorescent emitters: design tactics and applications in organic light-emitting diodes, *Chem. Soc. Rev.*, 2013, **42**(12), 4963–4976.
12 W. Wei, J. Li, D. Liu, Y. Mei, Y. Lan, H. Tian and B. Liu, Developing deep blue (CIE $y < 0.08$) and pure blue (CIE $y < 0.11$) OLEDs *via* molecular engineering of carbazole moiety, *New J. Chem.*, 2021, **45**(36), 16732–16739.
13 C. Adachi, Third-generation organic electroluminescence materials, *Jpn. J. Appl. Phys.*, 2014, **53**(6), 060101.
14 C. Bizzarri, F. Hundemer, J. Busch and S. Bräse, Triplet emitters versus TADF emitters in OLEDs: A comparative study, *Polyhedron*, 2018, **140**, 51–66.
15 U. Shakeel and J. Singh, Study of processes of reverse intersystem crossing (RISC) and thermally activated delayed fluorescence (TADF) in organic light emitting diodes (OLEDs), *Org. Electron.*, 2018, **59**, 121–124.
16 J. Gibson, A. P. Monkman and T. J. Penfold, The importance of vibronic coupling for efficient reverse intersystem crossing in thermally activated delayed fluorescence molecules, *Chem. Phys. Chem.*, 2016, **17**(19), 2956–2961.
17 N. Bunzmann, S. Weissenseel, L. Kudriashova, J. Gruene, B. Krugmann, J. V. Grazulevicius and V. Dyakonov, Optically and electrically excited intermediate electronic states in donor: acceptor based OLEDs, *Mater. Horiz.*, 2020, **7**(4), 1126–1137.
18 T. T. Bui, F. Goubard, M. Ibrahim-Ouali, D. Gigmes and F. Dumur, Recent advances on organic blue thermally activated delayed fluorescence (TADF) emitters for organic light-emitting diodes (OLEDs), *Beilstein J. Org. Chem.*, 2018, **14**(1), 282–308.
19 P. de Silva, C. A. Kim, T. Zhu and T. Van Voorhis, Extracting design principles for efficient thermally activated delayed fluorescence (TADF) from a simple four-state model, *Chem. Mater.*, 2019, **31**(17), 6995–7006.
20 B. A. Naqvi, M. Schmid, E. Crovini, P. Sahay, T. Naujoks, F. Rodella and W. Brütting, What controls the orientation of TADF emitters?, *Front. Chem.*, 2020, **8**, 750.
21 Y. Im and J. Y. Lee, Recent progress of green thermally activated delayed fluorescent emitters, *J. Inf. Disp.*, 2017, **18**(3), 101–117.
22 R. Braveenth and K. Y. Chai, Triazine-acceptor-based green thermally activated delayed fluorescence materials for organic light-emitting diodes, *Materials*, 2019, **12**(16), 2646.
23 H. Uoyama, K. Goushi, K. Shizu, H. Nomura and C. Adachi, Highly efficient organic light-emitting diodes from delayed fluorescence, *Nature*, 2012, **492**(7428), 234–238.
24 D. R. Lee, B. S. Kim, C. W. Lee, Y. Im, K. S. Yook, S. H. Hwang and J. Y. Lee, Above 30% external quantum efficiency in green delayed fluorescent organic light-emitting diodes, *ACS Appl. Mater. Interfaces*, 2015, **7**(18), 9625–9629.
25 Y. J. Cho, K. S. Yook and J. Y. Lee, High efficiency in a solution-processed thermally activated delayed-fluorescence device using a delayed-fluorescence emitting material with improved solubility, *Adv. Mater.*, 2014, **26**(38), 6642–6646.
26 M. Taneda, K. Shizu, H. Tanaka and C. Adachi, High efficiency thermally activated delayed fluorescence based on 1, 3, 5-tris (4-(diphenylamino) phenyl)-2, 4, 6-tricyanobenzene, *Chem. Commun.*, 2015, **51**(24), 5028–5031.
27 H. Tanaka, K. Shizu, H. Miyazaki and C. Adachi, Efficient green thermally activated delayed fluorescence (TADF) from a phenoxazine–triphenyltriazine (PXZ–TRZ) derivative, *Chem. Commun.*, 2012, **48**(93), 11392–11394.
28 W. L. Tsai, M. H. Huang, W. K. Lee, Y. J. Hsu, K. C. Pan, Y. H. Huang and C. C. Wu, A versatile thermally activated delayed fluorescence emitter for both highly efficient doped and non-doped organic light emitting devices, *Chem. Commun.*, 2015, **51**(71), 13662–13665.
29 Y. Wada, K. Shizu, S. Kubo, K. Suzuki, H. Tanaka, C. Adachi and H. Kaji, Highly efficient electroluminescence from a

solution-processable thermally activated delayed fluorescence emitter, *Appl. Phys. Lett.*, 2015, **107**(18), 105_1.

30 H. Kaji, H. Suzuki, T. Fukushima, K. Shizu, K. Suzuki, S. Kubo and C. Adachi, Purely organic electroluminescent material realizing 100% conversion from electricity to light, *Nat. Commun.*, 2015, **6**(1), 1–8.

31 R. Braveenth, H. Lee, S. Kim, K. Raagulan, S. Kim, J. H. Kwon and K. Y. Chai, High efficiency green TADF emitters of acridine donor and triazine acceptor D–A–D structures, *J. Mater. Chem. C*, 2019, **7**(25), 7672–7680.

32 C. C. Peng, S. Y. Yang, H. C. Li, G. H. Xie, L. S. Cui, S. N. Zou and L. S. Liao, Highly efficient thermally activated delayed fluorescence *via* an unconjugated donor–acceptor system realizing EQE of over 30%, *Adv. Mater.*, 2020, **32**(48), 2003885.

33 R. Ansari, W. Shao, S. J. Yoon, J. Kim and J. Kieffer, Charge Transfer as the Key Parameter Affecting the Color Purity of Thermally Activated Delayed Fluorescence Emitters, *ACS Appl. Mater. Interfaces*, 2021, **13**(24), 28529–28537.

34 H. Cho, C. W. Joo, S. Choi, C. M. Kang, B. H. Kwon, J. W. Shin and N. S. Cho, Organic light-emitting diode structure for high color gamut in high-resolution microdisplay: Over 90% color gamut based on BT, *Org. Electron.*, 2020, **101**, 106419.

35 I. Lee and J. Y. Lee, Molecular design of deep blue fluorescent emitters with 20% external quantum efficiency and narrow emission spectrum, *Org. Electron.*, 2016, **29**, 160–164.

36 T. Hatakeyama, K. Shiren, K. Nakajima, S. Nomura, S. Nakatsuka, K. Kinoshita and T. Ikuta, Ultrapure blue thermally activated delayed fluorescence molecules: efficient HOMO–LUMO separation by the multiple resonance effect, *Adv. Mater.*, 2016, **28**(14), 2777–2781.

37 J. M. Teng, Y. F. Wang and C. F. Chen, Recent progress of narrowband TADF emitters and their applications in OLEDs, *J. Mater. Chem. C*, 2020, **8**(33), 11340–11353.

38 K. C. Pan, S. W. Li, Y. Y. Ho, Y. J. Shiu, W. L. Tsai, M. Jiao and M. T. Lee, Efficient and tunable thermally activated delayed fluorescence emitters having orientation-adjustable CN-substituted pyridine and pyrimidine acceptor units., *Adv. Funct. Mater.*, 2016, **26**(42), 7560–7571.

39 T. L. Wu, M. J. Huang, C. C. Lin, P. Y. Huang, T. Y. Chou, R. W. Chen-Cheng and C. H. Cheng, Diboron compound-based organic light-emitting diodes with high efficiency and reduced efficiency roll-off, *Nat. Photonics*, 2018, **12**(4), 235–240.

40 Y. Xiang, P. Li, S. Gong, Y. H. Huang, C. Y. Wang, C. Zhong and C. Yang, Acceptor plane expansion enhances horizontal orientation of thermally activated delayed fluorescence emitters, *Sci. Adv.*, 2020, **6**(41), eaba7855.

41 Y. Chen, D. Zhang, Y. Zhang, X. Zeng, T. Huang, Z. Liu and L. Duan, Approaching nearly 40% external quantum efficiency in organic light emitting diodes utilizing a green thermally activated delayed fluorescence emitter with an extended linear donor–acceptor–donor structure, *Adv. Mater.*, 2021, **33**(44), 2103293.

42 J. Wang, N. Li, Q. Chen, Y. Xiang, X. Zeng, S. Gong and Y. Liu, Triarylboron-cored multi-donors TADF emitter with high horizontal dipole orientation ratio achieving high performance OLEDs with near 39% external quantum efficiency and small efficiency Roll-off, *Chem. Eng. J.*, 2022, **450**, 137805.

43 Y. Zhang, D. Zhang, J. Wei, Z. Liu, Y. Lu and L. Duan, Multi-resonance induced thermally activated delayed fluorophores for narrowband green OLEDs, *Angew. Chem., Int. Ed.*, 2019, **58**(47), 16912–16917.

44 Y. Zhang, D. Zhang, J. Wei, X. Hong, Y. Lu, D. Hu and L. Duan, Achieving pure green electroluminescence with CIEy of 0.69 and EQE of 28.2% from an aza-fused multi-resonance emitter, *Angew. Chem.*, 2020, **132**(40), 17652–17656.

45 Y. Xu, C. Li, Z. Li, J. Wang, J. Xue, Q. Wang and Y. Wang, Highly efficient electroluminescent materials with high color purity based on strong acceptor attachment onto b–n-containing multiple resonance frameworks, *CCS Chemistry*, 2022, **4**(6), 2065–2079.

46 Y. Xu, C. Li, Z. Li, Q. Wang, X. Cai, J. Wei and Y. Wang, Constructing Charge-Transfer Excited States Based on Frontier Molecular Orbital Engineering: Narrowband Green Electroluminescence with High Color Purity and Efficiency, *Angew. Chem., Int. Ed.*, 2020, **59**(40), 17442–17446.

47 M. Yang, I. S. Park and T. Yasuda, Full-color, narrowband, and high-efficiency electroluminescence from boron and carbazole embedded polycyclic heteroaromatics, *J. Am. Chem. Soc.*, 2020, **142**(46), 19468–19472.

48 M. Yang, S. Shikita, H. Min, I. S. Park, H. Shibata, N. Amanokura and T. Yasuda, Wide-Range Color Tuning of Narrowband Emission in Multi-resonance Organoboron Delayed Fluorescence Materials through Rational Imine/Amine Functionalization, *Angew. Chem., Int. Ed.*, 2021, **60**(43), 23142–23147.

49 P. Jiang, J. Miao, X. Cao, H. Xia, K. Pan, T. Hua and C. Yang, Quenching-Resistant Multiresonance TADF Emitter Realizes 40% External Quantum Efficiency in Narrowband Electroluminescence at High Doping Level, *Adv. Mater.*, 2022, **34**(3), 2106954.

50 Y. Zhang, G. Li, L. Wang, T. Huang, J. Wei, G. Meng and L. Duan, Fusion of Multi-Resonance Fragment with Conventional Polycyclic Aromatic Hydrocarbon for Nearly BT. 2020 Green Emission, *Angew. Chem., Int. Ed.*, 2022, e202202380.

51 X. F. Luo, S. Q. Song, H. X. Ni, H. Ma, D. Yang, D. Ma and J. L. Zuo, Multiple-Resonance-Induced Thermally Activated Delay Fluorescence Materials Based on Indolo [3,2,1-jk]-carbazole with an Efficient Narrowband Pure-Green Electroluminescence, *Angew. Chem., Int. Ed.*, 2022, **61**, e202209984.

52 J. Liu, Y. Zhu, T. Tsuboi, C. Deng, W. Lou, D. Wang and Q. Zhang, Toward a BT.2020 green emitter through a combined multiple resonance effect and multi-lock strategy, 2022, DOI: **10.21203/rs.3.rs-1357408/v1**.

53 Y. Liu, X. Xiao, Z. Huang, D. Yang, D. Ma, J. Liu and J. You, Space-Confined Donor-Acceptor Strategy Enables Fast Spin-Flip of Multiple Resonance Emitters for Suppressing Efficiency Roll-Off, *Angew. Chem.*, 2022, **61**, e202210210.

54 G. Liu, H. Sasabe, K. Kumada, A. Matsunaga, H. Katagiri and J. Kido, Facile synthesis of multi-resonance ultra-pure-green TADF emitters based on bridged diarylamine derivatives for efficient OLEDs with narrow emission, *J. Mater. Chem. C*, 2021, **9**(26), 8308–8313.

55 J. J. Hu, X. F. Luo, Y. P. Zhang, M. X. Mao, H. X. Ni, X. Liang and Y. X. Zheng, Green multi-resonance thermally activated delayed fluorescence emitters containing phenoxazine units with highly efficient electroluminescence, *J. Mater. Chem. C*, 2022, **10**(2), 768–773.

56 T. Hua, L. Zhan, N. Li, Z. Huang, X. Cao, Z. Xiao and C. Yang, Heavy-atom effect promotes multi-resonance thermally activated delayed fluorescence, *Chem. Eng. J.*, 2021, **426**, 131169.

57 F. Liu, Z. Cheng, Y. Jiang, L. Gao, H. Liu, H. Liu and W. Yang, Highly Efficient Asymmetric Multiple Resonance Thermally Activated Delayed Fluorescence Emitter with EQE of 32.8% and Extremely Low Efficiency Roll-Off, *Angew. Chem., Int. Ed.*, 2022, **61**(14), e202116927.

58 W. Yang, N. Li, J. Miao, L. Zhan, S. Gong, Z. Huang and C. Yang, Simple Double Hetero [5] helicenes Realize Highly Efficient and Narrowband Circularly Polarized Organic Light-Emitting Diodes, *CCS Chemistry*, 2022, 1–9.

59 Y. Yang, N. Li, J. Miao, X. Cao, A. Ying, K. Pan and C. Yang, Chiral Multi-Resonance TADF Emitters Exhibiting Narrowband Circularly Polarized Electroluminescence with an EQE of 37.2%, *Angew. Chem.*, 2022, **61**, e202202227.

60 N. Ikeda, S. Oda, R. Matsumoto, M. Yoshioka, D. Fukushima, K. Yoshiura and T. Hatakeyama, Solution-processable pure green thermally activated delayed fluorescence emitter based on the multiple resonance effect, *Adv. Mater.*, 2020, **32**(40), 2004072.

61 S. Oda, T. Sugitani, H. Tanaka, K. Tabata, R. Kawasumi and T. Hatakeyama, Development of Pure Green Thermally Activated Delayed Fluorescence Material by Cyano Substitution, *Adv. Mater.*, 2022, 2201778.

62 G. Liu, H. Sasabe, K. Kumada, H. Arai and J. Kido, Nonbonding/Bonding Molecular Orbital Regulation of Nitrogen–Boron–Oxygen-embedded Blue/Green Multiresonant TADF Emitters with High Efficiency and Color Purity, *Chem. – Eur. J.*, 2022, **28**, e202201605.

63 D. Sun, S. M. Suresh, D. Hall, M. Zhang, C. Si, D. B. Cordes and E. Zysman-Colman, The design of an extended multiple resonance TADF emitter based on a polycyclic amine/carbonyl system, *Mater. Chem. Front.*, 2020, **4**(7), 2018–2022.

64 F. Huang, K. Wang, Y. Z. Shi, X. C. Fan, X. Zhang, J. Yu and X. H. Zhang, Approaching efficient and narrow RGB electroluminescence from D–A-type TADF emitters containing an identical multiple resonance backbone as the acceptor, *ACS Appl. Mater. Interfaces*, 2021, **13**(30), 36089–36097.